**Atmospheric
Chemistry
and Physics
Discussions**

The unique properties of agricultural aerosols measured at a cattle feeding operation

N. Hiranuma[1,*], S. D. Brooks[1], J. Gramann[1], and B. W. Auvermann[2]

[1]Department of Atmospheric Sciences, Texas A&M University, 3150 TAMU, College Station, Texas 77843-3150, USA
[2]Texas AgriLife Research, 6500 Amarillo Blvd W.,Amarillo, Texas 79106, USA
[*]now at: Atmospheric Sciences and Global Change Division, Pacific Northwest National Laboratory, 902 Battelle Boulevard, Richland, WA 99352, USA

Correspondence to: S. D. Brooks (sbrooks@ariel.met.tamu.edu)

Discussion Paper | Discussion Paper | Discussion Paper | Discussion Paper

ACPD

11, 14417–14453, 2011

Agricultural aerosols measured at a cattle feeding operation

N. Hiranuma et al.

Title Page

Abstract	Introduction
Conclusions	References
Tables	Figures

◄ | ►

◄ | ►

Back | Close

Full Screen / Esc

Printer-friendly Version

Interactive Discussion

Abstract

Housing roughly 10 million head of cattle in the United States alone, open air cattle feedlots represent a significant but poorly constrained source of atmospheric particles. Here we present a comprehensive characterization of physical and chemical properties of particles emitted from a large representative cattle feedlot in the Southwest United States. In the summer of 2008, measurements and samplings were conducted at the nominally upwind and downwind edges of the facility. A series of far-field measurements and samplings was also conducted 3.5 km north of the facility. Two instruments, a GRIMM Sequential Mobility Particle Sizer (SMPS) and a GRIMM Portable Aerosol Spectrometer (PAS), were used to measure particle size distributions over the range of 0.01 to 25 µm diameter. Raman microspectroscopy (RM) was used to determine the chemical composition of particles on a single particle basis. Volume size distributions of fugitive dust were dominated by coarse mode particles. Twenty-four hour averaged concentrations of PM_{10} (particulate matter with a diameter of 10 µm or less) were as high as 1200 µg m^{-3} during the campaign. The primary constituents of the particulate matter were carbonaceous materials, such as humic acid, water soluble organics, and less soluble fatty acids, including stearic acid and tristearin. A significant percentage of the organic particles, up to 28 %, were composed of internally mixed with salts. Basic characteristics such as size distribution and composition of agricultural aerosols were found to be different than the properties of those found in urban and semi-urban aerosols. Failing to account for such differences will lead to serious errors in estimates of aerosol effects on climate, visibility, and public health.

1 Introduction

Increases in the size and number of concentrated animal feeding operations have led to increase in public concern regarding the emission of atmospheric pollutants, including gas phase and particulate matter (PM) emissions. Emissions of aerosol particles from

animal feeding operations have long been known to affect local air quality, visibility, and worker health (Gibbs et al., 2004; Priyadarsan et al., 2005; Rule et al., 2005; Upadhyay et al., 2008; Schicker et al., 2009). Volatile and semi-volatile compounds emitted with the particles are transported from feedlots throughout the nearby region, as evidenced by degraded air quality and unpleasant odors (Goetz et al., 2008; Occhipinti et al., 2008). Gaseous emissions from livestock include methane, ammonia, and nitrogen oxides (NRC, 2003; Aneja et al., 2008; Denmead et al., 2008; Ro et al., 2009; Hiranuma et al., 2010). To date, there is a surprising lack of particulate measurements at open-air animal facilities considering that agricultural fugitive dust represents a significant source of particles in certain locations (NRC, 2003; Hiranuma et al., 2008, 2010). In addition, to capture diurnal and seasonal cycles and the response of particulate concentrations to atmospheric conditions and precipitation, time- and size-resolved particulate measurements are needed in open-air cattle facilities.

Measurements of physical and chemical properties of aerosols are needed to assess the impacts of agricultural particles on visibility, radiative properties, climate, and human health. For instance, to assess health concerns, accurate measurements of PM_{10} (particles with aerodynamic diameters of $\leq 10\,\mu m$ or less) and $PM_{2.5} (\leq 2.5\,\mu m)$ are required to determine whether conditions meet national limits for air quality set by the US Environmental Protection Agency (EPA). The primary national limits, set to protect the health of sensitive populations including asthmatics, children, and the elderly, are $150\,\mu g\,m^{-3}$ and $35\,\mu g\,m^{-3}$, for 24-h averaged mass concentrations of PM_{10} and $PM_{2.5}$, respectively. Knowledge of particle concentrations are needed to evaluate health concerns specific to those individuals who work at the feedlots and those who live in feedlot neighborhoods (Von Essen and Auvermann, 2005). In one study of particle size distributions from dairy farming operations in California, high concentrations of coarse particles were observed (Nieuwenhuijsen et al., 1998). This led to the implementation of new operational procedures, including adding a cabin to the tractor to limit human exposure.

Agricultural aerosols measured at a cattle feeding operation

N. Hiranuma et al.

For a complete understanding of the issues surrounding agricultural aerosols, their chemical composition as well as physical properties must be known. A number of studies have shown that chemical composition of particles plays a key role in changing its physical properties, such as particle size and hygroscopicity (Brooks et al., 2003, 2004; Badger et al., 2006; Evelyn et al., 2009). In an airborne characterization of the particles downwind of a major bovine source in California, in situ measurements showed that organics comprised the dominant fraction of the total mass of submicron particles collected in the plume (Sorooshian et al., 2008). At a swine facility, the organic fraction of mass in particles was found to vary with particle size (Martin et al., 2008). In that study, up to 54 % of the fine particles contained organic materials, whereas the coarse size range contained less organic carbon (20 %) and relatively more minerals and inorganic salts.

Raman microspectroscopy (RM) is a powerful technique combining Raman spectroscopy and an optical microscope to determine the composition of atmospheric aerosols on a single particle basis (Tripathi et al., 2009; Sinanis et al., 2011). The Raman method provides detailed identification of a wide range of inorganic salts, water soluble organics, black carbon, soil, and biogenic materials in samples spanning the full size range of ambient aerosols (Sadezsky, et al., 2005; Ivleva et al., 2007; Mansour and Hickey, 2007; Tripathi et al., 2009). Further, RM can be used to create chemical maps of multiple components and to assess the degree of internal mixing in single particles. In a previous study, Raman microscopy and associated chemical mapping techniques were applied for the quantitative analysis and characterization of soot and related carbonaceous materials as well as the degree of graphitic structural order in airborne particulate matter collected with an electrical low pressure impactor (Ivleva et al., 2007).

Here we present observations of the physical and chemical properties of atmospheric particles collected at a representative open-air cattle feedlot in the Texas Panhandle. By conducting measurements at the nominally upwind edges and downwind of the facility as well as 3.5 km farther downwind of the facility, we have collected a

data set that provides insight on particulate transport on local and regional scales. Additional measurements of gaseous and particulate ammonia concentrations and the atmospheric extinction of agricultural particles were also conducted at the same facility (Hiranuma et al., 2008, 2010; Upadhyay et al., 2008).

2   Experimental

During July 2008, we conducted a two-week measurement campaign at an open air feedlot in Swisher County, TX, referred to here as Feedlot C. This feedlot, which houses 45 000 cattle in 1 square mile, is one of the ∼90 000 feedlots with 200 or more cattle scattered throughout the US (USDA, 2011; Upadhyay et al., 2008). Cattle feeding operations in Texas and Oklahoma annually market more than 3 million cattle, accounting for 28 % of the nation's fed cattle production as of February, 2011 (USDA, 2011).

Instruments used for particle size distribution measurement and size-resolved particle collection for off-line Raman microspectroscopy are shown in Fig. 1. A GRIMM Sequential Mobility Particle Sizer (SMPS) and a GRIMM Portable Aerosol Spectrometer (PAS) were operated together to measure size distributions over the broad range of 0.01 to 25 μm diameter. A PIXE Streaker mounted in a protective instrument housing beside the GRIMM instruments was used for continuous collection of particles. The particle size distributions and samples were collected ∼2 m above the ground at the nominally upwind and downwind edges of the facility. We also conducted a third series of "far-field" samples from the edge of a dirt road 3.5 km downwind of the feedyard.

During the field campaign, atmospheric conditions were monitored using an on-site HOBO 10-channel weather station (Model H21-001). This was deployed on a ∼2 m platform at the nominally downwind site to provide measurements of relative humidity, wind direction, ambient temperature, wind speed, and rainfall, recorded every six seconds. In addition, measurements of soil moisture and soil temperature at the surface and at a depth of 25 cm within the soil were obtained at the downwind sample site. As discussed below, surface soil moisture is a determining factor in the concentrations

of atmospheric dust events. Observations of meteorological and soil parameters are presented in Fig. 2. As can be seen in the figure, diurnal cycling was observed in all of the meteorological parameters. Throughout the project, wind direction was generally southerly with fluctuations between southwest and southeast directions. During the evening of 12 July, an abrupt shift to winds from the north was observed, causing variations in particle concentrations as discussed below. Similar shifts occurred on July 15th and very briefly on 19 July. In soil water content, an abrupt increase was observed on 15 July, due to heavy precipitation, followed by a gradual decrease until the end of the project.

2.1 Particle size distributions

The Sequential Mobility Particle Sizer consists of a Differential Mobility Analyzer (Model DMA-L) and an Ultrafine Particle Counter (Model 5.403). The SMPS records a full particle size distribution from 0.01 to 0.5 µm diameter by scanning the 39 size bins in this range every 7 min. Prior to entering the DMA, a stream of particles passes through a bipolar charger acquiring a well constrained charge distribution. Within the DMA, particles are classified according to their electrical mobility diameter, which is defined as the diameter of a spherical particle which would have the same electrical mobility as the particle of interest. In the case of spheres, the electrical mobility diameter is equal to the volume equivalent diameter. The second sizing instrument, the PAS, is a light scattering instrument which employs a 780 nm diode laser to measure the optical diameter of particles. The PAS records particle concentrations in 15 size bins in the range 0.3 to 25 µm optical diameter every 6 s. For a spherical particle, the optical diameter is identical to the volume equivalent diameter (Peters et al., 2006). Thus, if we assume the particles are spherical, the measurements of the SMPS and PAS can be combined directly to create a full size distribution, from 0.01 to 25 µm every 7 min collected at the nominally downwind site throughout the project.

During field measurements, particles were collected 2 m above the ground. Particles were passed through 1.8 m of inlet tubing, including 0.9 m of stainless steel tubing with

an inner diameter of 0.95 cm (3/8 inch), a 0.6 m long diffusion dryer and a 0.3 m length of conductive tubing with an inner diameter of 0.64 cm (1/4 inch) to reach the SMPS system. The diffusion dryer ensured a relative humidity below 5 % upon entry to the SMPS. Early tests indicated no change in the dryer relative humidity observed in 24 h of operation. Throughout the project, the desiccant in the dryer was changed daily. Prior to the field campaign, particle loss tests through the extended inlet tubing and desiccant drier in the size range of 50 nm to 25 μm were carried out by using known sizes of polystyrene latex with the TSI Atomizer (Model 3076) and the TSI Vibrating Orifice Aerosol Generator (Model 3450) in our laboratory. Unfortunately, substantial losses of more than 50 % of the particles in the sizes of 10 μm diameter and larger were observed by the PAS when sampling through the SMPS's extended inlet system and desiccant drier. In contrast, losses in fine mode aerosol measured by the SMPS were less than 15 %. To minimize the loss of coarse particles, we operated the PAS without the extended inlet and desiccant drier during all field measurements. Based on previous characterization of the low hygroscopicity of ambient particles at this feedlot, the size difference in coarse particles under ambient and dry conditions is 2 % at the most (Hiranuma et al., 2008).

An additional PAS was used to alternatively provide the upwind and far-field measurements. The upwind measurements were collected nearly continuously, with periodic interruptions for surveys of the far-field location. The far-field measurements were conducted for ∼2 h periods in the afternoons, beginning at ∼04:00 p.m. central daylight savings time and in the evenings, beginning at ∼10:00 p.m. To target the plume centerline, each far-field survey began with a series of eight PAS samples collected at prescribed far-field locations along the dirt road. The location of maximum concentration was interpreted as the plume centerline, and the PAS was returned to that point and operated for 10 min. The observed variability in aerosol transport to the far-field location is discussed in the section below. Pre- and post-campaign laboratory tests confirmed that the two PAS instruments were in agreement to within ±3 % in each bin size throughout the campaign.

2.2 Filter collection of particles

The PIXE Streaker is a filter sampler used to collect time resolved particulate samples for offline analysis by Raman microspectroscopy. Samples were collected at the downwind, upwind and far-field locations. The Streaker produces a continuous series of dis-
5 crete samples for offline chemical composition analyses on 82-mm diameter aluminum discs. Sampling intervals of 15 min were chosen. The 15-min sampling time resulted in intentionally low coverage of particles on the impaction stages suitable for the single particle Raman analysis described below. Prior to sampling, the foil was cleaned by rinsing with acetone (Sigma Aldrich, $\geq$99.5% purity) and drying at room temperature.
10 With an air flow of 1 l min^{-1}, particles were collected in the approximate size range of 2.5 to 10 µm aerodynamic diameter. Using an optical microscope, we later observed that a number of particles on the filters were outside the specified size ranges on the Streaker impaction stage. Several factors including turbulence, inconsistent flow rate, and irregular shape and density of agricultural dust may have contributed to the lack of
15 a distinct size cut-off point in the sampling (Kavouras and Koutrakis, 2001). All samples collected in the field were transported in a refrigerated cooler to Texas A&M University and stored under refrigeration at $-18\,^\circ$C until analysis by RM could be completed.

2.3 Raman microspectroscopy

A Thermo Fisher Scientific DXR Raman Spectrometer, equipped with an Olympus BX
20 microscope and a CCD detector, was used to probe single particle composition. A frequency doubled Nd:YVO$_4$ diode pumped solid state laser was used for excitation at 532 nm. For this study, an excitation laser power of 8 mW, an illumination time of 10 s, a 50× objective, and a 25 µm confocal aperture were chosen for all measurements. Spectra of the particulate samples were recorded over the range of 50 to 3500 cm^{-1}.
25 The Raman apparatus was equipped with a motorized stage that moves automatically in the x and y directions. Peaks in the Raman spectra of agricultural particles and their functional group assignments are summarized in Table 1.

Agricultural aerosols measured at a cattle feeding operation

N. Hiranuma et al.

By moving the stage in incremental 5 µm steps and taking a spectrum at each step, a spectral map of the sample could be created. For the coarse mode samples analyzed here, the mapping was performed over three 45 × 45 µm (2025 µm^2) areas on each impaction substrate. Based on typical coverage of field samples, most spectra represented a single independent particle. Occasionally, a few agglomerations were observed which were large enough to be detected in multiple spectra. We have developed a detailed strategy categorizing single particle data collected by RM. A summary of the results are presented below.

3 Results

3.1 Particle concentrations and size distributions

The GRIMM SMPS and PAS instruments collect data in 59 size bins ranging from 0.01 to 25 µm diameter, with both instruments nominally overlapping in the range of 0.3 to 1.0 µm diameter. Since the SMPS proved to be unreliable for particle sizes of 0.5 to 1.0 µm diameter (the last 5 bins of data), we report PAS data in this range. During the default scanning mode of the SMPS, the instrument scans the particle size range by starting at the highest voltage (largest particle size) and incrementally decreasing the voltage in a stepwise scan. Thus, the lowest voltage corresponding to the smallest particles is the last step in a scan, and is directly followed by the highest voltage of the following scan. If even a small fraction of fine particles (often present in orders of magnitude higher number concentration than larger particles) are not properly flushed from the system, they will be included in the count obtained at high voltage and may account for a major fraction of the observed large particle concentration. To test this, we generated ammonium sulfate particles with the TSI atomizer and directed the sample flow to the SMPS. Reported concentrations of coarse particles were much higher than expected from atomizer operation. Next, the SMPS was held at a single voltage, corresponding to the largest size. Over a period of minutes, the concentrations

of particles dropped to zero. This was repeated for the all bins. Results showed the SMPS overcounted particles in the largest 5 bins, 0.5 to 1.0 μm diameter, when operated in the default fast scanning mode. Since our field sampling was conducted in this mode, SMPS measurements in those bins are not reported here. Fortunately, the PAS
5 measurements covered this size range.

To illustrate the uniqueness of the particle population in the vicinity of a major cattle feeding operation, we briefly consider particle volume distributions collected with the PAS and the SMPS in the three sites: in downtown Houston, TX, in the semi-urban town of College Station (home to Texas A&M University), and at Feedyard C on the Texas
10 Panhandle. The particle size distributions for each site averaged over a 24 h period are shown in Fig. 3. The areas below the curves in 3a, 3b, and 3c correspond to the total particle number, surface area, and volume concentration, respectively. While these are only snapshots of the data collected from each location, they illustrate the extreme differences in size distributions present in urban, semi-urban and agricultural sites (Yin
15 et al., 2008). Concentrations of fine particles are lower at the feedlot than in other locations. In contrast, the coarse particle mode at the cattle feeding facility contains at least two orders of magnitude more particles than in the urban and rural settings. At the facility, the surface area distribution peaks in a mode at ∼10 μm diameter. The volume distribution is also dominated by large particles.

20 Next we present a time series of the hourly averaged volume concentrations of particles measured by the SMPS in the range of 0.01 to 0.5 μm diameter and PAS instrument in the range of 0.3 to 25 μm diameter at the downwind and upwind edges of the facility for the duration of the campaign period, shown in Fig. 4. These data were obtained by converting the observed number concentration in each size bin to volume,
25 assuming that all particles were spheres with diameters equal to the average diameter in the bin. The EPA uses the mass of particles in two size ranges, PM_{10} and $PM_{2.5}$, as the metrics for assessing the health issues due to inhalation. We note that our measurement technique differs from the approved EPA standard measurement in two ways. First, we measured particle size, rather than mass. Second, our PAS instrument

is a measurement of optical diameter, whereas the standard measurement involves measuring the mass of particles sized according to their aerodynamic diameter. In the case of a sphere, the optical and aerodynamic diameters are both equivalent to a sphere's geometric diameter. However, for nonspherical particles, optical and aerodynamic diameters deviate from the geometric diameter in different ways, depending on particle size, shape, and density. Despite these differences, our measurements can be used to estimate the PM_{10} and $PM_{2.5}$ levels. Further, our concentration data confirmed the need for EPA standardized methods appropriately tailored to the aerodynamics of these coarse, irregularly shaped agricultural particles, as previously observed by Buser et al. (2007a, b).

To obtain an estimated PM_{10} volume concentration, we summed the particle counts in the 12 PAS bins up to and including 10 µm diameter. As can be seen in Fig. 4a, the peak downwind volume concentrations observed by PAS were extremely high, $\sim 1 \times 10^{13}\, nm^3\, cm^{-3}$. The upwind concentrations were typically much lower, with values up to as $6.1 \times 10^{11}\, nm^3\, cm^{-3}$. Interestingly, the major peaks occurred in the evenings, unlike the diurnal cycles of urban particle populations. Evenings at the feedlot are characterized by cooler temperatures, higher relative humidities, and lower wind speeds. The observed peaks may be driven by two concurrent changes occurring in the evenings. First, it is well known that as air cools, the height of the boundary layer is reduced (Baum et al., 2008). Thus particles emitted at or near ground level are confined to a smaller mixed layer resulting in higher concentrations within that layer. Second, we routinely observed that the cattle became more active in the cooler evening air. This is possibly a homeostatic behavior due to the accumulation of metabolic energy from feeding earlier in the day. In fact, this behavior is well known in the cattle feeding industry, and daily evening increases in cattle activity have been well documented by others (Auvermann et al., 2000). The hoof action of the active cattle pulverizes and lofts the dry manure into the air contributing to increased dust concentrations in the evenings (Razote et al., 2006).

We also observed a sudden drop in the concentration of atmospheric coarse particles following precipitation. Intense rain fell continuously from 01:00 a.m. to 04:00 a.m. on 15 July 2008 resulting in 6.3 mm of accumulated precipitation and causing a sudden drop in particle concentration. Cleaner atmospheric conditions persisted until the rain stopped and the pen surface dried out on 18 July 2008, as signified by the return to soil moisture conditions of less than 0.2 vol/vol (Smettem, 2006). Afterwards, the diurnal cycling of coarse particulate concentrations were once again observed. The diurnal cycle had a second, less dramatic feature in the mornings, coincident with routine morning feeding at the facility.

Next, if we assume the concentration of particles at the upwind site (depending on the wind direction of the day) is solely due to background aerosol, we can estimate the fraction of the total aerosol attributed to feedlot activities by subtracting this background contribution from the downwind volume concentrations. These background-corrected measurements are shown in Fig. 4b for the total PAS size range (0.3 to 25 μm). Similarly, we present background-corrected volume concentrations of PM_{10} in Fig. 4b. To consider the fine mode particles from the feedlot, we summed up the all particles with diameters up to and including 2.0 μm, since the PAS does not have a bin cut-off at exactly 2.5 microns. We refer to this as the volume concentration of $PM_{2.0}$ (Fig. 4b), and consider it to be a lower limit to the volume concentration of $PM_{2.5}$. During the field campaign, the concentration of coarse particles (PM_{10}) derived from the feedlot was typically two orders of magnitude higher than that measured at the upwind site, indicating that the feedlot emissions are by far the dominant source of local coarse particles. Exceptions to this occurred in three brief periods during the campaign, on 12, 15 and 19 July when the winds shifted to northerly flow. Since the upwind and downwind sites are essentially reversed under northerly flow conditions, the background-corrected aerosol volumes at the nominally downwind site appear to be negative at these times.

Due to proximity to the source, we acknowledge that the upwind measurements most likely contained at least some contribution from the feedlot as well. For coarse particles, the diurnal cycle observed downwind of the facility was mimicked at the upwind site,

Agricultural aerosols measured at a cattle feeding operation

N. Hiranuma et al.

Full Screen / Esc

Printer-friendly Version

Interactive Discussion

suggesting that the upwind site was influenced by particle contributions from the feedlot. Observed PM_{10} concentrations at the downwind edge of the lot were extremely high and as discussed below, and represent a potential concern for health and regional air quality. Unlike the coarse mode, fine mode concentrations from the facility accounted for only roughly half (∼56 %) of the ambient $PM_{2.0}$.

We next consider the details of variations in volume size distributions for a segment of data collected on 18 to 25 July 2008, as shown in Fig. 5. We include a shortened segment of the time series here in order to view changes in time in greater detail. These days included the diurnal variations occurring under typical dry conditions, from 20 to 25 July 2008, as well as the transition from wet to dry conditions after the rainfall on 16 July. As seen in Fig. 5a, we observed a distinct diurnal cycle with maximum concentrations of 1-h averaged total PAS counts (10^{13} nm^3 cm^{-3}) occurring at 09:00 p.m. in the evenings at the downwind edge of the facility. Volume size distributions at the nominally upwind site are shown in Fig. 5b. The persistent diurnal cycle included particles in all sizes down to 0.5 µm diameter. Below 0.5 µm diameter, there was not a pronounced diurnal cycle. At the upwind location, particle distributions were much more variable. At this site, volume contributions from the coarse and fine modes were similar; whereas at the downwind site, the coarse mode clearly dominated.

The fine mode was more randomly variable than the coarse mode throughout the 15-day measurement period. Observed fine mode concentrations appeared to be influenced by feedings as well as less routine activity at the feedlot including pen cleaning, grass cutting, delivery of grain, and milling of grain into feed in the on-site mill. The high concentrations of fine PM observed at the upwind location may have been triggered by preceding cleaning activity, daily arrival and departure of the cattle truck, and associated feedlot activities. These activities usually happened on the south side of the feedlot during morning and afternoon hours. On 23 July 2008, elevated levels of fine mode concentrations coincided with grass cutting activities at the upwind location. The downwind total PM concentrations typically exceeded upwind ones. An exception was observed during a period in the evening of 12 July when northerly winds dominated

(Fig. 2). During this period, the hourly averaged PM concentration was as high as $6.1 \times 10^{11}\,\mathrm{nm^3\,cm^{-3}}$ at the nominally upwind location (Fig. 4a).

Additional measurements were periodically conducted at a far-field location, 3.5 km downwind of the field. For example, the particulate plume on 22 July evening is illustrated in Fig. 5c and 5d. Figure 5c shows an expanded time period from 5a, shown for 1 h of data. Figure 5d shows the far-field measurements for the same period of time. During this time, wind speed ($2.4 \pm 0.5\,\mathrm{m\,s^{-1}}$), and wind direction (from the south $149 \pm 8°$) were fairly constant. Under these conditions, the time for an air mass to travel from the feedlot to the far-field was ~30 min. The total PAS concentrations measured at the downwind edge of the field and the far-field location were $5.8 \times 10^{12}\,\mathrm{nm^3\,cm^{-3}}$ and $3.5 \times 10^{11}\,\mathrm{nm^3\,cm^{-3}}$, respectively. As one might expect, a significant drop in the mean size of the transported aerosol was observed. The volume distribution in the plume shifted to smaller sizes with distance downwind from the plume source (from 10 to 15 μm at the downwind site to 2 to 7.5 μm at the far-field site, depending on particle concentration at the source, wind speed, and deposition velocity). For example, if we estimate that a population of particles larger than 5 μm diameter has a deposition velocity of $5\,\mathrm{cm\,s^{-1}}$ and a mixing depth of 50 m near the surface, only 16 % would be observed after 30 min and less than 3 % would remain after 1 h (Herner et al., 2006).

Unlike the coarse particle concentrations, concentrations of fine mode particles at the far-field site were consistently >99 % of those at the facility. In fact, far-field concentrations occasionally exceeded the fine PM measured at the facility, even under steady southerly wind conditions. Rainfall enhances microbial activity in soil leading to increases in concentrations of ammonia and fine particles (Pruppacher and Klett, 1997; Hiranuma et al., 2010). One day after the rainstorm of 15 July, the total particle load was reduced. However, an increase of 25 % in fine mode particle volume was observed at the far-field site. In contrast, during the hot and dry conditions of 20 July and later, soil moisture returned to <0.2 vol/vol and the fine mode concentrations at the far-field location were consistently ≤7.5 % of those measured at the edge of the feedlot. While coarse mode particles are a more significant local issue, fine mode

particulates are more efficiently transported regionally. Fine mode contributions to the particle population are less significant in volume than the coarse mode, but will extend over a greater area and may weigh heavily in regional assessments of air quality.

To summarize the potential health effects of PM derived from the feedlot, we estimated the mass concentrations from the feedlot based on our measurements. Direct measurements have been converted to volume as described above. Since we do not have a direct measurement of particle density, we considered converting volume to mass three ways, using the density of airborne dust, $1.71\,\mathrm{g\,cm^{-3}}$, compacted feedlot soil, $2.65\,\mathrm{g\,cm^{-3}}$, and water, $1.0\,\mathrm{g\,cm^{-3}}$ (Sweeten et al., 1998; Smettem, 2006). We consider the density of dust to be the best estimate, and soil and water as upper and lower limits to the actual density, respectively. The daily averages of PM_{10} and $PM_{2.0}$ mass concentrations at the nominal downwind location as function of time are shown in Fig. 6a and b. As can be seen in Fig. 6a, at the downwind edge of the facility, 24-h average PM_{10} mass concentrations were as high as $\sim 1200\,\mathrm{\mu g\,m^{-3}}$ (assuming the mass density of dust). To put the observed mass concentrations in context, we note that the limit of the maximum allowable exposure set by the primary US EPA under the National Ambient Air Quality Standard (NAAQS) for PM_{10} is $150\,\mathrm{\mu g\,m^{-3}}$ (24-h average). Observed mass concentrations were higher than the NAAQS limit ($150\,\mathrm{\mu g\,m^{-3}}$ for 24-h average) for most of the campaign period (11 out of 15 days, assuming the mass density of dust). Although our measurements cannot be used to provide a standard EPA assessment, these results suggest that feedlots may be a significant source of PM_{10}, and additional assessment of PM_{10} at feedlots should be conducted. In contrast, the observed mass of $PM_{2.0}$ was consistently much lower (Fig. 6b). The highest observed mass concentration of $PM_{2.0}$, $45\,\mathrm{\mu g\,m^{-3}}$, occurred on 23 July 2008. This was the only day that the observed mass was higher than $35\,\mathrm{\mu g\,m^{-3}}$ (24-h average), the NAAQS limit for $PM_{2.5}$. Grass cutting activities observed on this day may have contributed to the higher concentration of smaller particles measured.

3.2 Characterization of chemical compositions

Aerosol composition has been observed on single particle basis using Raman microspectroscopy. Since RM is a high resolution but labor intensive technique, only a total of 10 filter samples were analyzed. Representative samples from the upwind, downwind, and far field locations were included. These samples were collected on two dusty days, 22 and 24 July 2008, characterized by high concentrations of particles and dry conditions.

During RM sample analysis, an optical microscope was used to focus on a 50 µm by 50 µm gridded area on the filter. A CCD camera collected and recorded an image such as the one shown in Fig. 7a. A Raman spectrum was collected at each of the point grid on the microscope map, as indicated by the red points in the figure. The spectra collected on three individual particles in the image (labeled I, II, and III) are shown in Fig. 7b. As can been seen, the composition varied from particle to particle. Particle I was an internal mixture of organics and calcium nitrate, $Ca(NO_3)_2$. Particle II was even more complex and had all the components of Particle I plus calcium carbonate, $CaCO_3$. In contrast, Particle III had only one major feature, a broad band at $\sim 1500\,cm^{-1}$. This band indicated the presence of amorphous highly conjugated organic rings of carbon (Sadezky et al., 2005). Since Raman cannot distinguish for certain whether these peaks arise from brown carbon, i.e., soil and humic acid, or from black carbon or diesel soot, we refer to this peak as black or brown carbon or "BBC" (Escribano et al., 2001). BBC was found to be a major component of samples collected during this campaign as discussed in further detail below. The spectra collected at each point can be compiled to create a spectral map of total intensity as indicated by individual peak heights. For example, we generated maps of the peak heights at 1050, 1085 and $1500\,cm^{-1}$, corresponding to $CaCO_3$, $Ca(NO_3)_2$, and BBC, respectively (Fig. 7c). These maps illustrated the high degree of internal mixing within particles as well as the external mixing of particle types. Particle I was present in the first and third maps, of $Ca(NO_3)_2$ and BBC, respectively. With such a complex ensemble of particle compositions, a

Full Screen / Esc

Printer-friendly Version

Interactive Discussion

classification strategy was required to simplify and interpret the results. Our strategy for sorting particles into three major categories is described below.

Of 3000 spectra taken on 10 filters during the mapping procedure, 993 were collected on particles and had spectral features above the background. Six spectra could not be classified to due high fluorescence signal. The remaining spectra were categorized as BBC, smaller organic compounds, or inorganics, depending on the major component in their spectra (Fig. 8). Fluorescence can be caused by high concentrations of conjugated systems, found in aromatic rings present in biological materials (Mansour and Hickey, 2007). In these cases, the fluorescence signal overwhelmed the Raman spectra at all wavenumbers, making it impossible to identify the composition. Throughout the project, we observed a high degree of internal mixing in the particles. All peaks with intensities above 50 counts per second were considered major components and were used in the further sorting into subcategories. The results are shown in Table 2.

The average fractions of BBC, organics, and inorganics identified on given filters collected at the downwind edge of the feedlot were $52 \pm 12\%$, $44 \pm 11\%$ and $4 \pm 2\%$ (mean ± standard deviation), respectively (Table 2). The reported experimental uncertainties arose due to the nonlinear responses of various compounds to Raman excitation laser intensity. All spectra reported in this analysis were collected at 8.0 mW. However, to test the variations of excitation laser intensity, we also collected spectra at 4.0 mW and 1.0 mW on samples of known compositions and test samples collected in the field. For most organic categories, we observed decreases in the height of characteristic peaks with a decrease in laser intensity. However, for humic acid, we observed the opposite trend. As the excitation intensity was decreased from 8 mW to 1 mW, the broad band at 1050 to 1620 cm^{-1} increased by 34 %. Also, the characteristic terpenoid peaks at 1154 and 1513 cm^{-1} were observed in test samples only when an excitation intensity of 4 mW or less was used. Decomposition of terpenoids could explain the disappearance of the peak at 8 mW. Since our standard analysis was conducted at 8.0 mW, we must conclude that this analysis was insensitive to any terpenoids present in the samples and possibly other semivolatile compounds as well. It should also be

noted that potassium chloride and sodium chloride, which we identified in our previous study of elemental composition analysis of agricultural particles from the same cattle feedlot, are not Raman active (Batonneau et al., 2006; Hiranuma et al., 2008).

More than half of the particles at the feedlot contained BBC. Since the sources and optical properties of black and brown carbon are quite different, it would clearly be desirable to differentiate between them. In an effort to elucidate more subtle spectral differences, we collected spectra on samples of known compositions, including humic acid from Fluka Chemical Co., Pahokee Peat and Leonardite humic acids obtained from the International Humic Acid Substances Society, a soot sample generated by burning propane in our laboratory, and graphite from the tip of a No. 2 lead pencil (Fig. 9). While the highly ordered graphite sample was clearly unique in that it has the sharpest peaks, the other spectra were quite similar to one another. Others have observed that depending on type of fuel and degree of oxidation, anthropogenic soot samples can be even more disordered than humic materials (Sadezky, 2005; Ivleva, 2007). Thus, we conclude that there is no spectral evidence that the BBC observed in this study is derived entirely from soil samples. However, given the location, soil-derived humic materials, manure, and road dust are the most plausible sources of the majority of the BBC in these samples collected in this project.

The second largest category of particles was comprised of smaller organic compounds, including a wide variety of water soluble compounds, including aromatic compounds, alcohols, and amines. At times as many as 20 % of the organic spectra were fatty acids, including stearic acid and tristearin. During the period of the highest observed concentrations of fatty acids, the morning of 22 July, on-site grinding of hay and flaking of grain into cattle feed were occurring during sample collection. Previous studies have shown that aerosols containing fatty acids are generated by both processing of feed and lofting of dried dust from the soil (Rogge et al., 2006).

On average, ~4 % of the spectra from samples collected at the downwind location were identified as purely inorganics, as compared to ~13 % at the upwind edge of the facility. While very few particles contained purely inorganics, a significant number

did contain salts internally mixed with BBC or other organics. At both the upwind site and downwind locations, as much as ~28 % of all samples contained internally mixed organics and inorganic salts. Specific inorganic compounds observed in this study included calcium nitrate, sodium nitrate, and calcium carbonate. Calcium and sodium are used as additives in the diet fed to the cattle and are also present in the unpaved road dust (Buchanan et al., 1996; Ocsay et al., 2006). Minor fractions of other salts and mineral dust constituents, listed in Table 1, were also identified in the field samples (Ansari and Pandis, 1999; Zweifel et al., 2001).

The abundance of organic material in particles at Feedlot C was unusually high for atmospheric aerosols. Taken together, BBC and organics were present in more than 90 % of the samples. Even in samples collected at the upwind edge of the facility, more than ~80 % contained organics. It is interesting to note that, that the composition of $PM_{2.5}$ observed in rural areas is typically dominated by ammonium sulfate and ammonium nitrate (Malm et al., 2004). According to nationwide IMPROVE network measurements of $PM_{2.5}$, increased levels of organic materials are more typically observed in areas closer to urban centers (Malm et al., 2004). While present in lower quantities than the organics, inorganics still play a significant role in determining the fate of the predominately coarse particles analyzed here. Many of the organics present here including brown or black carbon, fatty acids, and surfactant molecules have low hygroscopicity. In these cases, the presence of deliquescent salts may facilitate water uptake by these particles (Hiranuma et al., 2008).

As summarized in Table 2 and Fig. 8, the composition of particles at the upwind edge of the feedlot was somewhat different than downwind samples. However, even at this edge, the particle composition was still predominately influenced by feedlot activities, which overwhelmed the background aerosol signal. Also, no compositional variation between the downwind edge of the facility and 3.5 km away was observed. This indicates that particles from the feedlot are transported regionally. In addition, no notable variations were observed in the samples collected in the morning, afternoon, and evening, though composition measurements of more samples than included here

would be needed to refine analysis of any potential diurnal cycles. In short, the feedlot supplied a large contribution of mainly organic particles that varied diurnally in physical properties while remaining fairly constant in composition.

4   Conclusions

Aerosols have impacts on air quality and human health as well as on scattering and absorption of sunlight and climate. While vast efforts have been made to characterize urban anthropogenic particulate emissions, efforts in agricultural settings are lacking. This study represents the most comprehensive investigation of the chemical and physical properties of particles at a representative cattle feeding operation to date. As our results indicate, aerosols emitted from the feedlot are unique in size, concentration, composition, and diurnal cycle compared to those emitted in other urban and rural locations. Thus, these unique characteristics must be accounted for future emission inventory at feedlots.

Two instruments, a GRIMM SMPS and a GRIMM PAS Model 1.108 were employed simultaneously to survey the particle population in the range of 0.01 to 25 micron diameter. A unique feature of particles from the feedlot was the diurnal cycle. Under dry conditions at the feedlot, a maximum in coarse mode concentrations was routinely reached during the evenings (~09:00 p.m.). We observed extremely high atmospheric loadings of hourly averaged PM measured by PAS, up to $10^{13}\,\mathrm{nm^3\,cm^{-3}}$. Two factors, increased cattle activity and decreased boundary layer height, may have contributed to the high concentrations routinely observed in the evenings relative to the rest of the day. A second feature of the diurnal cycle was a smaller peak occurring in the mornings during feeding times.

Size distribution measurements showed the coarse particulates dominate the particulate volume concentrations. Strikingly, the coarse particle mode routinely observed at the feedlot contained two orders of magnitude more particles than typically observed in urban and rural locations. With an estimated daily averaged PM_{10} as high as ~1200 µg m^{-3}, particle concentrations were consistently above the NAAQS primary

Full Screen / Esc

Printer-friendly Version

Interactive Discussion

health limit for PM_{10} of daily average limit of $150\,\mu g\,m^{-3}$. While PM_{10} was a concern on site at the facility, our far-field measurements of PM concentration indicated rapid decay with downwind distance. In fact, measured ground-level PM_{10} concentrations 3.5 km beyond the edge of the facility were reduced to ∼8.5 % of concentrations on-site. While
5 coarse particle loadings decreased rapidly with distance from the source, fine mode particulates were more efficiently transported. Thus, fine mode contributions to the particle population are less significant in mass, but will extend over a greater spatial area and must be included in regional assessments of air quality.

In addition to physical measurements, offline measurements of single particle com-
10 position were performed using Raman microspectroscopy. The particles were largely organic in nature, the majority of which were classified as brown or black carbon. At the downwind edge of the facility, an average of 96 % of the particles contained organic material, 15 % contained internally mixed organics and inorganics, and 4 % contained exclusively inorganics. Even at the upwind edge of the facility, 87 % of particles con-
15 tained organics, 28 % contained internally mixed organics and inorganics, and only 13 % contained exclusively inorganics.

This study includes important results regarding the chemical and physical aspects of agricultural particles and the health concern they pose. Our analysis of particle size distributions and composition showed that agricultural particles represent a complex
20 mixture which differs in both physical and chemical properties from particle popula-tions in other locations. While on-site levels of PM_{10} were extremely high, a large frac-tion of the coarse particles was rapidly deposited, and thus the impacts of the coarse mode were lessened at the regional level. However, the significance of the fine and coarse modes emitted from cattle feeding operations should be included for accurate
25 assessments at the regional scale.

References

Aneja, V. P., Arya, S. P., Kim, D.-S., Rumsey, I. C., Arkinson, H. L., Semunegus, H., Bajwa, K. S., Dickey, D. A., Stefanski, L. A., Todd, L., Mottus, K., Robarge, W. P., and Williams, C. M.: Characterizing ammonia emissions from swine farms in eastern North Carolina: Part 1-conventional lagoon and spray technology for waste treatment, J. Air Waste Manage. Assoc., 58, 1130–1144, 2008.

Ansari, A. S. and Pandis S. N.: Prediction of multicomponent inorganic atmospheric aerosol behavior, Atmos. Environ., 33(5), 745–757, 1999.

Auvermann, B. W.: Lesson 42: Controlling dust and odor from open lots, edited by Koelsch, R. et al. Livestock and Poultry Environmental Stewardship (LPES) National Curriculum, Midwest Plan Service, 26 pp., Ames, IA, 2000.

Badger, C. L., George, I., Griffiths, P. T., Braban, C. F., Cox, R. A., and Abbatt, J. P. D.: Phase transitions and hygroscopic growth of aerosol particles containing humic acid and mixtures of humic acid and ammonium sulphate, Atmos. Chem. Phys., 6, 755–768, doi:10.5194/acp-6-755-2006, 2006.

Baum, K. A., Ham, J. M., Brunsell, N. A., and Coyne, P. I.: Surface boundary layer of cattle feedlots: implications for air emission measurement, Agr. Forest Meteorol., 148, 1882–1893, 2008.

Batonneau, Y., Sobanska, S., Laureyns, J., and Bremard, C.: Confocal microprobe Raman imaging of urban tropospheric aerosol particles, Environ. Sci. Technol., 40 1300–1306, 2006.

Brooks, S. D., Garland, R. M., Wise, M. E., Prenni, A. J., Cushing, M., Hewitt, E., and Tolbert, M. A.: Phase changes in internally mixed maleic acid/ammonium sulfate aerosols, J. Geophys. Res., 108(D15), 4487, doi:10.1029/2002JD003204, 2003.

Brooks, S. D., DeMott, P. J., and Kreidenweis, S. M.: Water uptake by particles containing humic materials and mixtures of humic materials with ammonium sulfate, Atmos. Environ., 38, 1859–1868, 2004.

Buchanan, J. S., Berger, L. L., Ferrell, C., Fox, D. G., Galyean, M., Hutcheson, D. P., Klopfenstein, T. J., and Spears, J.: Nutrient requirements of beef cattle: Subcommittee on Beef Cattle Nutrition, Committee on Animal Nutrition, Board on Agriculture, National Research Council, National Academy Press, Washington, DC, 1996.

Buser, M. D., Parnell Jr., C. B., Shaw, B. W., and Lacey, R. E.: Particulate matter sampler errors

Agricultural aerosols measured at a cattle feeding operation

N. Hiranuma et al.

Title Page

Abstract	Introduction
Conclusions	References
Tables	Figures

|◄ | ►|

◄ | ►

Back | Close

Full Screen / Esc

Printer-friendly Version

Interactive Discussion

due to the interaction of particle size and sampler performance characteristics: ambient PM_{10} samplers, Transactions of the ASAE, 50(1), 229–240, 2007a.

Buser, M. D., Parnell Jr., C. B., Shaw, B. W., and Lacey, R. E.: Particulate matter sampler errors due to the interaction of particle size and sampler performance characteristics: ambient $PM_{2.5}$ samplers, Transactions of the ASAE, 50(1), 241–254, 2007b.

Denmead, O. T., Chen, D., Griffith, D. W. T., Loh, Z. M., Bai, M., and Naylor, T.: Emissions of the indirect greenhouse gases NH_3 and NOx from Australian beef cattle feedlots, Australian Journal of Experimental Agriculture, 48, 213–218, 2008.

Escribano, R., Sloan, J. J., Siddique, N., Sze, N., and Dudev, T.: Raman spectroscopy of carbon-containing particles, Vibrational Spectroscopy, 26, 179–186. 2001.

Evelyn, J. F., Martin, S. T., and Buseck, P. R.: Deliquescence and efflorescence of potassium salts relevant to biomass-burning aerosol particles, Aerosol Sci. Technol., 43, 799–807, 2009.

Gibbs, S. G., Green, C. F., Tarwater, P. M., and Scarpino, P. V.: Airborne antibiotic resistant and nonresistant bacteria and fungi recovered from two swine herd confined animal feeding operations, Journal of Occupational and Environmental Hygiene, 1(11), 699–706, 2004.

Goetz, S., Aneja, V. P., and Zhang, Y.: Measurement, analysis, and modeling of fine particulate matter in eastern North Carolina, J. Air Waste Manage. Assoc., 58(9), 1208–1214, 2008.

Herner, J. D., Ying, Q., Aw, J., Gao, O., Chang, D. P. Y., and Kleeman, M. J.: Dominant mechanisms that shape the airborne particle size and composition in central California, Aerosol Sci. Technol., 40, 827–844, 2006.

Hiranuma, N., Brooks, S. D., Auvermann, B. W., and Littleton, R.: Using environmental scanning electron microscopy to determine the hygroscopic properties of agricultural aerosols, Atmos. Environ., 42, 1983–1994, 2008.

Hiranuma, N., Brooks, S. D., Thornton, D. C. O., and Auvermann, B. W.: Atmospheric ammonia mixing ratios at an open-air cattle feeding facility, J. Air Waste Manage. Assoc., 60, 210–218, 2010.

Ivleva, N. P., McKeon, U., Niessner, R., and Pöschl, U.: Raman microspectroscopic analysis of size-resolved atmospheric aerosol particle samples collected with an ELPI: Soot, humic-like substances, and inorganic compounds, Aerosol Sci. Technol., 41, 655–671, 2007.

Kavouras, I. G. and Koutrakis, P.: Use of polyurethane foam as the impaction substrate/collection medium in conventional inertial impactors, Aerosol Sci. Technol., 34, 46–56, 2001.

Title Page

Abstract | Introduction

Conclusions | References

Tables | Figures

|◄ | ►|

◄ | ►

Back | Close

Full Screen / Esc

Printer-friendly Version

Interactive Discussion

Malm, W. C., Schichtel, B. A., Pitchford, M. L. Ashbaugh, L. L., and Eldred, R. A.: Spatial and monthly trends in speciated fine particle concentration in the United States, J. Geophys. Res., 109, D03306, doi:10.1029/2003JD003739, 2004.

Mansour, H. M. and Hickey, A. J.: Raman characterization and chemical imaging of biocolloidal self-assemblies, drug delivery systems, and pulmonary inhalation aerosols: a review, AAPS PharmSciTech, 8(4) Article 99, E1–E16, 2007.

Martin, R. S., Silva, P. J., Moore, K., Erupe, M., and Doshi, V. S.: Particle composition and size distributions in and around a deep-pit swine operation, Ames, IA, J. Atmos. Chem., 59, 135–150, 2008.

National Research Council (NRC): Air Emissions from Animal Feeding Operations: Current Knowledge, Future Needs, Ad Hoc Committee on Air Emissions from Animal Feeding Operations, Committee on Animal Nutrition, NRC, 2003.

Nieuwenhuijsen, M. J., Kruize, H., and Schenker, M. B.: Exposure to dust and its particle size distribution in California agriculture, American Industrial Hygiene Association, 59(1), 34–38, 1998.

Occhipinti, C., Aneja, V. P., Showers, W., and Niyogi, D.: Back-trajectory analysis and source-receptor relationships: particulate matter and nitrogen isotopic composition in rainwater, J. Air Waste Manage. Assoc., 58(9), 1215–1222, 2008.

Ocsay, R., Salma, I., Wang, W., and Maenhaut, W.: Characterization and diurnal variation of size-resolved inorganic water-soluble ions at a rural background site, J. Environ. Monit., 8, 300–306, 2006.

Peters, T. M., Ott, D., and O'Shaughnessy, P. T.: Comparison of the Grimm 1.108 and 1.109 portable aerosol spectrometer to the TSI 3321 aerodynamic particle sizer for dry particles, Annals of Occupational Hygiene, 50(8), 843–850, 2006.

Priyadarsan, S., Annamalai, K., Sweeten, J. M., Holtzapple, M. T., and Mukhtar, S.: Co-gasification of blended coal with feedlot and chicken litter biomass, Proceedings of the Combustion Institute, 30, 2973–2980, 2005.

Pruppacher, H. R. and Klett, J. D.: Microphysics of clouds and precipitation, 2nd revised and enlarged edition, Kluwer, Academic Publishers, Dordrecht, The Netherlands, 225–229, 1997.

Razote, E. B., Maghirang, R. G., Predicala, B. Z., Murphy, J. P., Auvermann, B. W., Harner, J. P., and Hargrove, W. L.: Laboratory evaluation of the dust-emission potential of cattle feedlot surfaces. Transactions of the ASAE, 49(4), 1117–1124, 2006.

Ro, K. S., Johnson, M. H., Varma, R. M., Hashmonay, R. A., and Hunt, P.: Measurement of

greenhouse gas emissions from agricultural sites using open-path optical remote sensing method, J. Environ. Sci. Health Part A, 44(10), 1011–1018, 2009.

Rogge, W. F., Medeiros, P. M., and Simoneit, B. R. T.: Organic marker compounds for surface soil and fugitive dust from open lot dairies and cattle feedlots, Atmos. Environ., 40(1) 27–49, 2006.

Rule, A. M., Chapin, A. R., McCarthy, S. A., Gibson, K. E., Schwab, K. J., and Buckley, T. J.: Assessment of an aerosol treatment to improve air quality in a swine concentrated animal feeding operation (CAFO), Environ. Sci. Technol., 39(24), 9649–9655, 2005.

Sadezky, A., Muckenhuber, H., Grothe, H., Niessner, R., and Pöschl, U.: Raman microspectroscopy of soot and related carbonaceous materials: Spectral analysis and structural information, Carbon, 43 1731–1742, 2005.

Schicker, B., Kuhn, M., Fehr, R., Asmis, L. M., Karagiannidis, C., and Reinhart, W. H.: Particulate matter inhalation during hay storing activity induces systemic inflammation and platelet aggregation, European Journal of Applied Physiology, 105, 771–778, 2009.

Sinanis, S., Aleksandrova, M., and Schaber, K.: Characterization of Multicomponent Aerosols by Raman Spectroscopy, Aerosol Sci. Technol., 45(6), 741–747, 2011.

Smettem, K. R.: Particle Density, in Encyclopedia of Soil Science, edited by: Lal, R., Taylor & Francis, 2060 pp., London, England, 2006.

Sorooshian, A., Murphy, S. M., Hersey, S., Gates, H., Padro, L. T., Nenes, A., Brechtel, F. J., Jonsson, H., Flagan, R. C., and Seinfeld, J. H.: Comprehensive airborne characterization of aerosol from a major bovine source, Atmos. Chem. Phys., 8, 5489–5520, doi:10.5194/acp-8-5489-2008, 2008.

Sweeten, J. M., Parnell Jr., C. B., Shaw, B. W., and Auvermann, B. W.: Particle size distribution of cattle feedlot dust emission, Transactions of the ASAE, 41(5), 1477–1481, 1998.

Tripathi, A., Jabbour, R. E. Guicheteau, J. A., Christensen, S. T., Emge, D. K., Fountain, A. W., Bottiger, J. R., Emmons, E. D., and Snyder, A. P.: Bioaerosol analysis with Raman chemical imaging microspectroscopy, Anal. Chem., 81, 6981–6990, 2009.

Upadhyay, J., Auvermann, B. W., Paila, A. N., and Hiranuma, N.: Open-path transmissometry to determining the atmospheric extinction efficiency of feedyard dust, Transactions of the ASAE., 51(4), 1433–1441, 2008.

United States Department of Agriculture (USDA): Cattle on Feed, National Agricultural Statistics Service, ISSN: 1948–9080, 2009.

Von Essen, S. G. and Auvermann, B. W.: Health effects from breathing air near CAFOs for

Agricultural aerosols measured at a cattle feeding operation

N. Hiranuma et al.

Title Page

Abstract	Introduction
Conclusions	References
Tables	Figures

◄◄ ►►

◄ ►

Back | Close

Full Screen / Esc

Printer-friendly Version

Interactive Discussion

feeder cattle or hogs, Journal of Agromedicine, 10(4), 55–64, 2005.

Yin, J. X. and Harrison, R. M.: Pragmatic mass closure study for $PM_{1.0}$, $PM_{2.5}$ and PM_{10} at roadside, urban background and rural sites, Atmos. Environ., 42(5), 980–988, 2008.

Zweifel, H., Maier, R. D., and Schiller, M.: Plastics additives handbook 6th ed. Hanser, München, Germany, 2001.

Agricultural aerosols measured at a cattle feeding operation

N. Hiranuma et al.

Back | Close

Full Screen / Esc

Printer-friendly Version

Interactive Discussion

Table 1. Peak assignments for Raman shifts observed in this study.

Raman Peak Assignments	
Raman Shift, cm^{-1}	Organic Compounds[a,b]
150 to 425	skeletal deformation of CC aliphatic chains
480 to 525	S-S stretches of dialkyl sulfides
1200	disordered graphitic lattice (A_{1g} symmetry), polyenes, ionic impurities
1350	disordered graphitic lattice (A_{1g} symmetry)
1500	amorphous carbon, Black or Brown carbon (BBC)
1580	ideal graphitic lattice (E_{2g} symmetry)
1620	disordered graphitic lattice (E_{2g} symmetry)
2700 to 2850	CHO group vibration of aliphatic aldehydes
2849 to 3103	C-H, = (C-H), ≡ (C-H) stretches of alkane/alkene/aromatics
2986 to 2974	symmetric NH_3^+ stretch of aqueous alkyl ammonium chlorides
3154 to 3175	bonded NH stretch of pyrazoles
3145 to 3310	bonded NH/NH_2 stretch of amides
3250 to 3400	bonded symmetric NH_2 stretch of amines
3374	CH stretch of acetylene (gas)
3340 to 3380	bonded OH stretch of aliphatic alcohols
Raman Shift, cm^{-1}	Inorganic Compounds, major peaks, cm^{-1}[c]
976	ammonium sulfate
994	sodium sulfate
1006	calcium sulfate
1044	ammonium nitrate
1046	bisodium carbonate
1050	calcium nitrate
1069	sodium nitrate
1080	sodium carbonate
1088	calcium carbonate

[a,b] Organic chemical bond on the basis of Dollish et al. (1974) and Ivleva et al. (2007).

[c] For identification of Raman spectra (band wavenumbers and relative intensities) of inorganics, the resolved spectra are compared with commercially available spectral libraries (Thermo Scientific, Nicolet Instruments, Marcel Dekker Inc.).

Title Page

Abstract | Introduction

Conclusions | References

Tables | Figures

◄ | ►

◄ | ►

Back | Close

Full Screen / Esc

Printer-friendly Version

Interactive Discussion

Table 2. Chemical classification of particles collected at the indicated sampling locations and times.

Location & Time	Downwind Morning	Downwind Afternoon	Downwind Evening	Downwind Average	Upwind Evening	Far-Field Evening
Number of Recorded Spectra	364	127	211	234	133	158
High Fluorescence, %	1	1	0	0	0	2
I. Black or Brown Carbon (BBC)	61	39	56	52	33	47
i. BBC	24	23	17	21	5	26
ii. BBC + Organics	29	9	13	17	7	16
iii. BBC + Inorganic(s)	5	2	12	6	9	4
iv. BBC + Organics + Inorganic(s)	3	5	14	7	12	1
II. Organics, %	37	56	38	44	54	48
i. Fatty Acid [R-C(=O)OH]	20	1	3	8	3	3
ii. Other Organics	16	55	34	35	44	44
iii. Organics + Inorganic(s)	1	0	1	1	7	1
III. Inorganics, %	1	5	6	4	13	3
i. Inorganic	1	5	4	3	11	3
ii. Multiple Inorganics	0	0	2	1	2	0
Total Organic (I. BBC + II. Organics), %	98	94	94	96	87	96
Organic/Inorganic Internal Mixtures (I. iii. + I. iv. + II. iii.), %	10	6	28	15	28	6

Agricultural aerosols measured at a cattle feeding operation
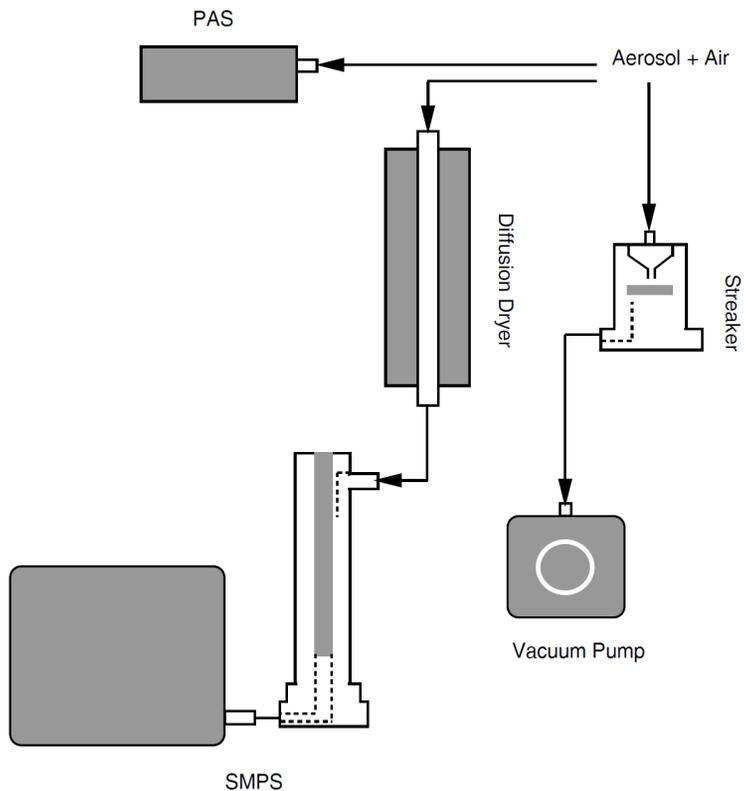
N. Hiranuma et al.

Fig. 1. Schematic of the field sampling apparatus.
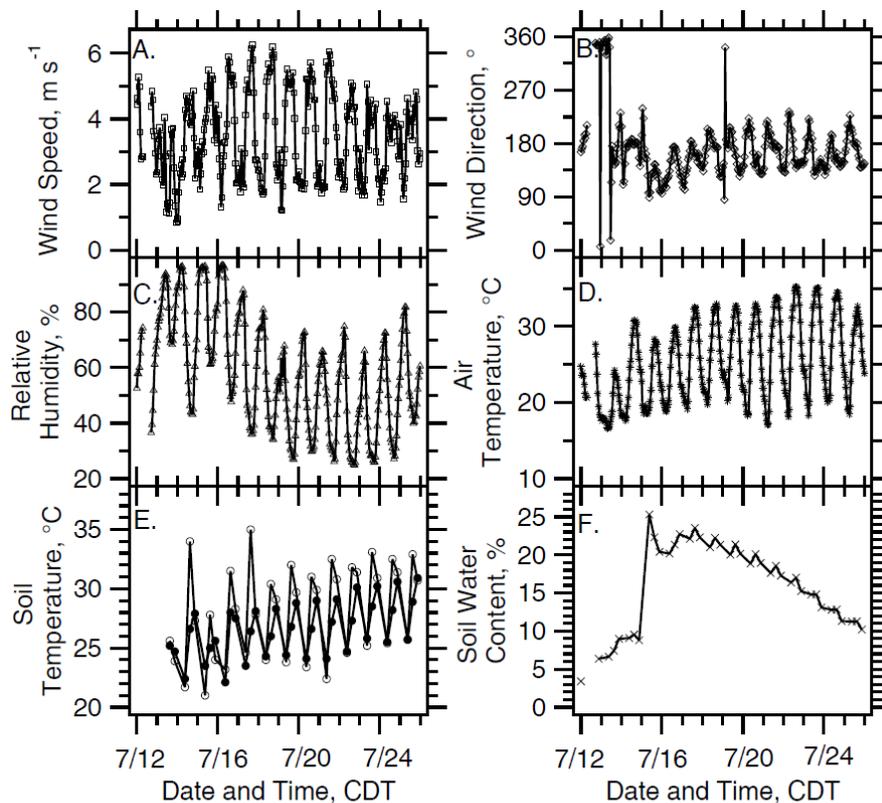
Fig. 2. Hourly averaged meteorological data including wind speed, wind direction, relative humidity, air temperature, soil temperature at a depth of 5 cm (open circles) and 25 cm (solid circles), and soil water content at a depth of 25 cm are shown in **(A–F)**, respectively (Adapted from Hiranuma et al., 2010).

Title Page

Abstract | Introduction

Conclusions | References

Tables | Figures

◄ | ►

◄ | ►

Back | Close

Full Screen / Esc

Printer-friendly Version

Interactive Discussion
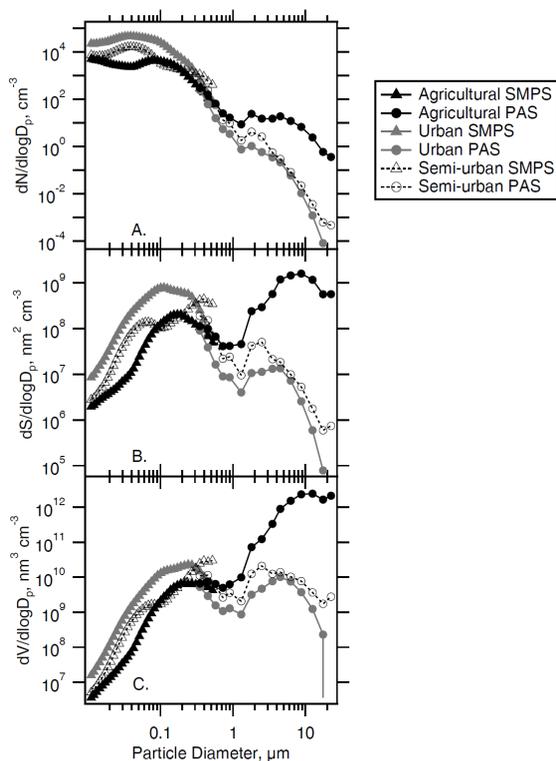
Fig. 3. Measured 24 h averaged aerosol number, surface area, and volume distributions are shown in **(A)**, **(B)**, and **(C)**, respectively. Distributions measured at an agricultural site (Feedyard C, TX) on 24 July 2008, and urban site (downtown Houston, TX) on 26 September 2006, and a semi-urban site (College Station, TX) on 16 June 2006 are indicated by the solid black, solid grey, and open black marks, respectively. Within each size distribution, aerosol measured by the SMPS (0.01 to 0.5 μm diameter) and the PAS (0.3 to 25 μm diameter) are shown as triangles and circles, respectively. Note that both axes are in log scale.
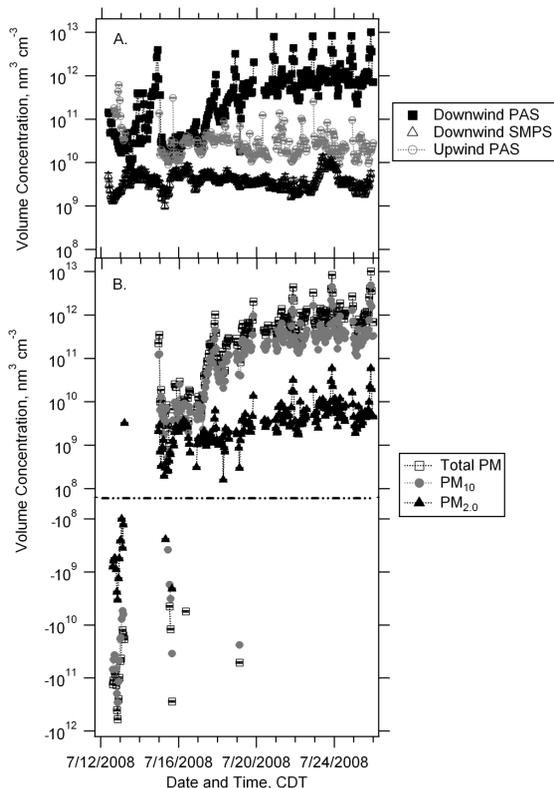
Fig. 4. In **(A)**, hourly averaged volume concentrations of PM measured by the PAS and the SMPS at the nominal downwind site and by the PAS at the upwind site are shown as solid squares, open triangles, and open grey circles, respectively. In **(B)**, background corrected feedlot particle concentrations (volume concentrations) of the total particles sampled by the PAS, of particles ≤10 μm diameter, and of particles ≤2.0 diameter are shown as open squares, solid grey circles, and solid triangles, respectively. Error bars represent measurement uncertainties of ±17 % and ±3 % for the SMPS and PAS, respectively.

Title Page

Abstract | Introduction

Conclusions | References

Tables | Figures

◄ | ►

◄ | ►

Back | Close

Full Screen / Esc

Printer-friendly Version

Interactive Discussion
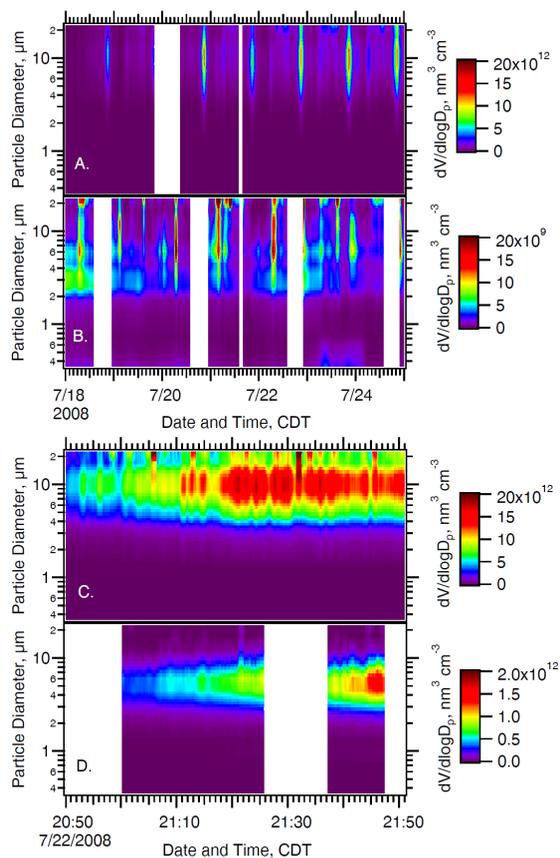
Fig. 5. Hourly averaged aerosol volume distributions measured at the downwind and upwind locations are shown in **(A)** and **(B)**, respectively. An expanded view of 1 h of data collected on 22 July from the downwind site is shown in **(C)**, and data collected at the far-field location in the same time period is shown in **(D)**.
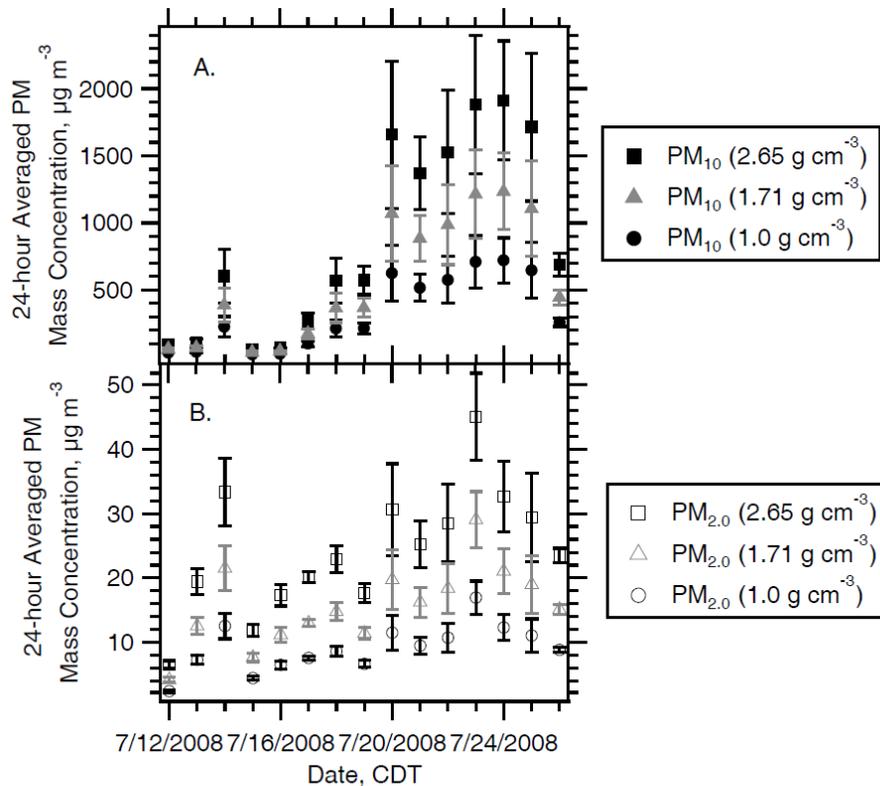
Fig. 6. Daily averaged mass concentrations of PM_{10} and $PM_{2.0}$ at the downwind location are shown in **(A)** solid and **(B)** open marks, respectively. Squares, triangles, and circles represent mass concentration assuming the particle density is equivalent to that of soil (2.65 g cm^{-3}), dust (1.71 g cm^{-3}), and water (1.0 g cm^{-3}), respectively. Error bars represent the standard error of the mean measured concentration over 24 h period.
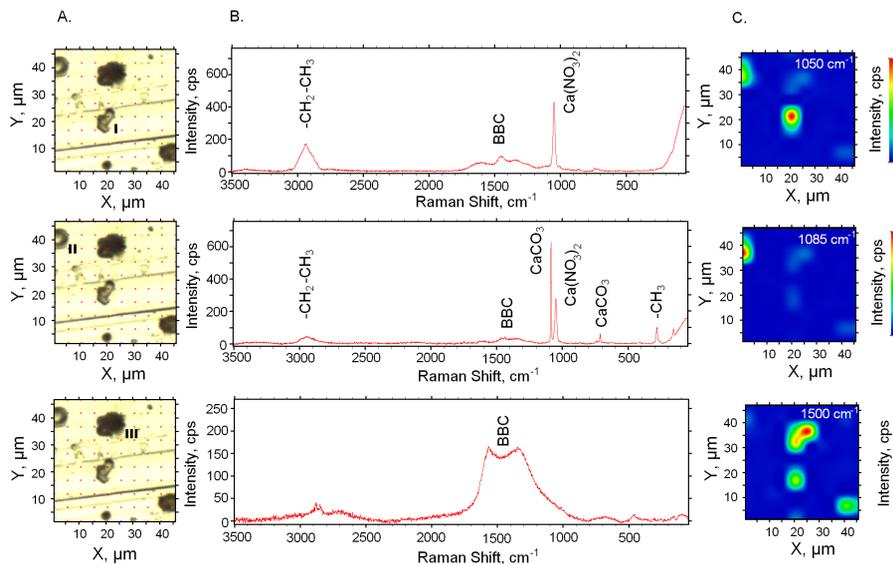
Fig. 7. In **(A)**, microscopic image of Particles I, II, and III collected from upwind location 22 July at ~09:00 p.m. In **(B)**, the full Raman spectra of Particle I, II, and III are shown. In **(C)**, spectral maps of major components of the particles are shown including Ca $(NO_3)_2$ at 1050 cm^{-1}, $CaCO_3$ at 1085 cm^{-1}, and black or brown carbon (BBC) at ~1500 cm^{-1}.
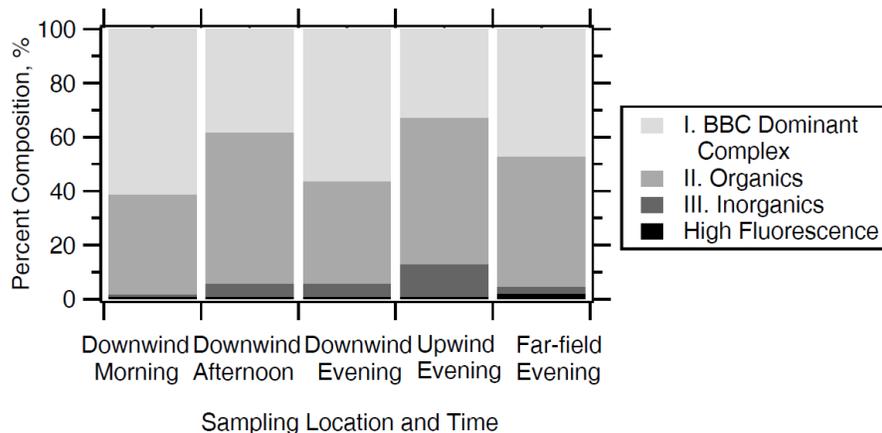
Fig. 8. The percentage of particles classified as each composition group are shown for samples collected at the downwind site in the morning, afternoon, and evening and at the upwind and far-field sites in the evening.
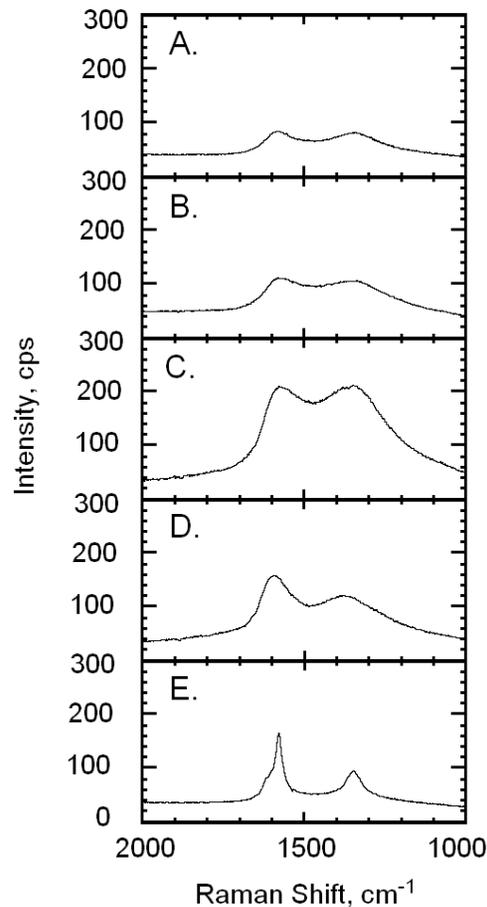
Fig. 9. Raman spectra of reference materials including **(A)** soot generated by burning propane gas in our laboratory, **(B)** Fluka humic acid, **(C)** Pahokee peat humic acid, **(D)** Leonardite humic acids, and **(E)** graphite are shown. Spectra are focused on the range of 1000 to 2000 cm^{-1}.